PHASE DISTORTIONS OF AN OPTICAL BEAM DUE TO ITS SELF-ACTION UNDER CONDITIONS OF GRAVITATIONAL CONVECTION

V.P. Lukin and B.V. Fortes

Institute of Atmospheric Optics,
Siberian Branch of the Academy of Sciences of the USSR, Tomsk
Received October 1, 1990

The process of gravitational convection which arises as a result of the heating of a gas by an optical beam as it propagates in a horizontally positioned cell with the square cross section is considered. A program which can be used to calculate the structure of the planar convective flow and the temperature distribution over the cross section of the cell has been developed. The operational efficiency of a modal and segmented mirror for correction of the phase distortions appearing during the propagation of the optical radiation in the radiation-induced thermal inhomogeneities is investigated.

The propagation of an intense coherent beair, in a horizontally oriented cell with the square cross section, filled with a weakly absorbing gas with absorption coefficient a, is considered. Heating of the gas occurs as a result of photoabsorption, and, under the action of the buoyancy forces, a motion of the heated volume toward the upper cell boundary starts. As the beam propagates in the radiation-induced thermal inhomogeneities, distortions of the radiation phase $\varphi = 2\pi / \lambda n'_T T$ appear, where λ is the wavelength, T is the temperature profile, and n'_T is the derivative of the refractive index with respect to the temperature.

The process of gravitational convection was previously studied in a qualitative way by the methods of similarity theory[1,2] and numerically.[4–6,9,10] In these studies, either the radiation beam, [1,2,5,6,9] or the elevated temperature of one of the cell walls[4,10] served as the heat source. Murokh[5] considered a cell with the circular cross section and solved the problem of beam propagation in the cell in the geometric-optics approximation. The phase distortions for the case of a cell with square cross section were calculated in Ref. 6, in which the beam propagation was described in the parabolic-equation approximation. In this paper, as in all those cited above, the convection is calculated in the planar—flow approximation, which corresponds to the case in which the cell length L is much greater than the effective beam radius a_0.

Mathematical formulation of the problem. The process of planar convective flow in the cell cross section in the Boussines approximation is described by the following system of equations[3,4]:

$$\frac{\partial T}{\partial t} + \frac{\partial \psi}{\partial y}\frac{\partial T}{\partial x} - \frac{\partial \psi}{\partial x}\frac{\partial T}{\partial y} = \frac{1}{\mathrm{Pr}}\left[\frac{\partial^2 T}{\partial x^2} + \frac{\partial^2 T}{\partial y^2}\right] + I(x, y); \tag{1}$$

$$\frac{\partial \omega}{\partial t} + \frac{\partial \psi}{\partial y}\frac{\partial \omega}{\partial x} - \frac{\partial \psi}{\partial x}\frac{\partial \omega}{\partial y} = \frac{\partial^2 \omega}{\partial x^2} + \frac{\partial^2 \omega}{\partial y^2} + \mathrm{Gr}\frac{\partial T}{\partial x}; \tag{2}$$

$$\frac{\partial^2 \psi}{\partial x^2} + \frac{\partial^2 \psi}{\partial y^2} + \omega = 0. \tag{3}$$

Here x and y are the horizontal and vertical coordinates, ψ is the stream function associated with the local flow velocity by the relations

$$V_x = \frac{\partial \psi}{\partial y}; \quad V_y = -\frac{\partial \psi}{\partial x}, \tag{4}$$

ω is the artificially introduced eddy function,[3,4] and T is the temperature of the medium. Equations (1)—(3) arewritten in dimensionless form. The variables which enter in them are scaled in the following way: the eddy and stream functions are scaled to $\psi_0 = \nu$ and $\omega_0 = \nu/l^2$, x and y to l, time to $t_0 = I^2/\nu$, and the temperature to T_0. The radiation intensity I is scaled to $I_0 = \rho T_0 C\nu/(al^2)$. The dimensionless combinations $\mathrm{Pr} = \nu/a$ and $\mathrm{Gr} = \rho g l^3 T_0/\nu^2\beta$ are the Prandtl number and the Grashof number, where ν is the kinematic viscosity, l is the transverse dimension of the cell, ρ is the density of the medium, $\beta = 1/\rho_0\partial\rho/\partial T$ is the volume expansion coefficient, g is the acceleration of free fall, a is the thermal conductivity, C is the heat capacity, and T_0 is the characteristic temperature drop. Since there is an uncertainty in the last parameter in the given formulation of the problem, it is possible to choose any value, for example, $T_0 = 1$°C.

The boundary conditions are specified in the following way:

for the temperature

$$T(x, y)\big|_b = 0, \tag{5}$$

and for the stream function

$$\psi\big|_b = 0; \quad \frac{\partial \psi}{\partial n}\Big|_b = 0. \tag{6}$$

0235-6880/90/12 1182-4 $02.00

Here, the index "b" refers to the boundary line of the cell cross section, and n is the normal to the boundary line. The boundary condition for $\partial\psi/\partial n$ makes it . possible to obtain the boundary values of the eddy function.

Numerical method. A uniform square grid $(x_{i,j})$, where $i, j = \overline{0, N}$ and the step $h = 1/N$, was specified over the cell cross section. For the temperature and stream functions, null boundary conditions were prescribed on the grid boundaries, and as—Woods boundary condition was employed for the eddy function.[4,11,12]

The symmetric location of the heat source with respect to the vertical axis of the cross section makes it necessary to solve the problem for only half the grid. An implicit scheme[4] which is a version of the method of variable directions was used to solve Eqs. (1) and (2). The solution of the equation according to this scheme is performed by the pass technique. The Poisson equation (3) was solved by expanding in a double sine series.[7] A mixed-radix FFT algorithm,[13] which allows one to vary the computational grid size within wide limits, was used to calculate the sine-transform.

Calculation of the temperature profile. The temperature profile was assumed to follow the form of the Gaussian beam

$$I(x, y) = I_c \exp\{-[(x - 1/2)^2 + (y - 1/2)^2]/a_0^2\}. \quad (7)$$

The effective radius of the beam a_0 scaled to l was equal to $a_0 = 0.075$. The rest of the parameters of the problem were as follows: Pr = 1, Gr = 10, the time step Δt was chosen from the condition $\Delta t V_y^{\max} = h$, where $V_y^{\max}$ is the amplitude of the vertical component of the convective flow velocity, and the beam power

$$P = \iint_{-1/2}^{1/2} I(x, y)\,dx\,dy \quad (8)$$

varied within the limits 10^{-3}–10^{3}. The dynamics of the two-dimensional fields T, ψ, and ω was calculated on a PC and visualized using interactive graphics.

With the radiation power increased to 10^3 the convective flow velocity grows by roughly another factor of 10, as a result of which a complex multivortex flow structure is formed.

For low radiation power, e.g., $P = 10^{-3}$, the effect of the thermal conductivity factor already becomes noticeable from the very beginning of the evolution of the convective process, and, as a result, the isothermal contours smooth out, and the process rapidly relaxes as a result of an intense heat exchange with the cell walls.

For intermediate radiation power, e.g., $p = 1$, the thermal conductivity is manifested much more weakly and at later stages of the process since the convective flow velocity is increased by approximately a factor of ten. In this connection, the thermal conductivity factor is manifested for the most part only at the stage at which the heated gas flows along the inner wall surfaces. Relaxation occurs with the attainment of a balance between the heat source power and the rate of heat exchange with the cell walls.

The radiation power thus affects the structure of the two-dimensional temperature profile $T(x, y)$ and especially the structure of the convective flow, characterized by the field ψ. This effect, however, is, perceptible only for a very significant change in the beam power, since the velocity of the convective process depends on the power like $P^{1/3}$.

From the viewpoint of estimating the phase distortions and of the possibility of their compensation, the variation of the mode structure of the distortions of the phase of the optical radiation $\phi(x, y)$, which is proportional to the two-dimensional profile $T(x, y)$, is of interest. In order to perform such an estimation, the standard deviation of the profile T from its mean value over the beam cross section was calculated

$$\sigma_T = \left\{ \frac{1}{4\pi a_0^2} \int_S\int (T(x, y) - T_m)^2 dx\,dy \right\}^{1/2}. \quad (9)$$

where S is a circle of radius $2a_0$ with its center located on the beam axis and T_m is the mean temperature over S. The value σ_T is equal to the standard deviation of the phase on the circle S to within a constant factor. Below, with the help of. a program which imitates the phase corrector operation, the distortions of the field T which remain after correcting the predistortions by the corrector are computed, and then the standard deviation σ_T^C, which characterizes the residual phase distortions, is calculated from a formula identical to formula (9). The dependences of the ratio σ_T^C / σ_T on the time after switching on the beam for various variants of the phase corrector are plotted in Figs. 1–3.

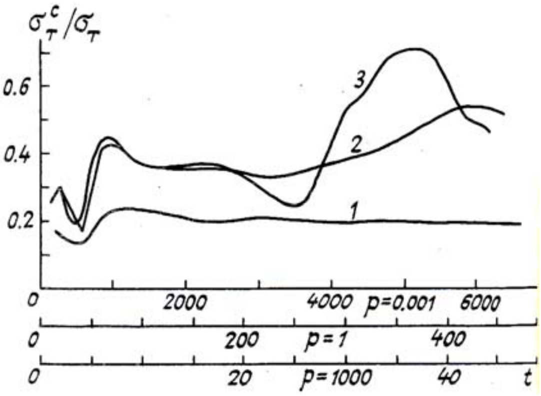

FIG. 1.

The residual distortions vs time after switching the beam on for three values of P (0.001, 1, and 1000) are plotted in Fig. 1. The normalized time values in all the figures must be multiplied by a factor of 10^{-5} to give the actual time in seconds. The curves in Fig. 1 are calculated for the case of a mode corrector which compensates for the classical aberrations from tilt to spherical aberration, inclusive. It can be seen that the residual distortions increase as the power increases, that is, the spectrum of the phase distortions is shifted toward higher aberrations. In addition, these curves illustrate the increase in the amplitude of the fluctuations of the parameters of the convective process with increase in the beam power.

The dynamics of the residual phase distortions for the radiation power $P = 1$ in correcting for the following classical aberrations: 1) tilt, 2) tilt and defocusing, 3) tilt, defocusing, and astigmatism, 4) tilt.

The dynamics of the residual distortions in the case of a segmented seven-element corrector with a hexagonal configuration of the segments is plotted in Fig. 3. Curve 1 corresponds to correction of the mean phase within every segment, while curve 2 corresponds to compensation for the mean phase and the total tilt within every segment. In the latter case, the efficiency of the segmented corrector differs hardly at all from that of the modal corrector, which corrects all the aberrations up to spherical, inclusive (curve 5 in Fig. 2).

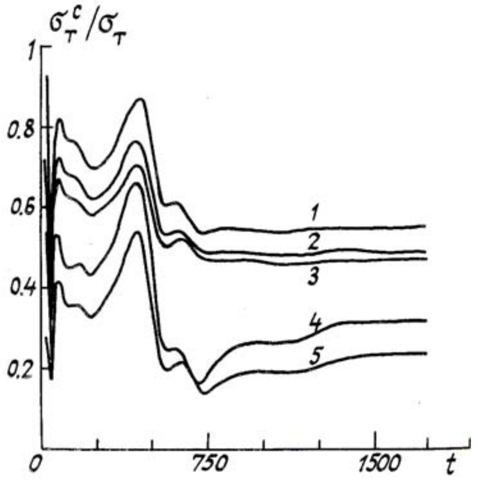

FIG. 2.

Finally, it may be noted that am efficient program which makes it possible to calculate and visualize (on an interactive display) the dynamics of the planar convective flow which appears during the propagation of an intense beam in a horizontally positioned cell with rectangular cross section has been created. The operational efficiency of the modal and segmented correctors for correcting the phase distortions produced as the beam propagates through the radiation-induced defocusing, astigmatism, and coma, and 5) from tilt- to spherical aberration, inclusive, is plotted in Fig. 2. It can be seen that the tilt comprises up to 40% of the distortions, and the coma comprises about 20%. In this figure, in contrast to Fig. 1, relaxation can be seen, since a longer time interval is plotted, thermal inhomogeneities has been investigated. In contrast to Ref. 6, in which the mode structure of such distortions was also studied, we have found that the phase distortion spectrum shifts toward higher aberrations as the radiation power increases.

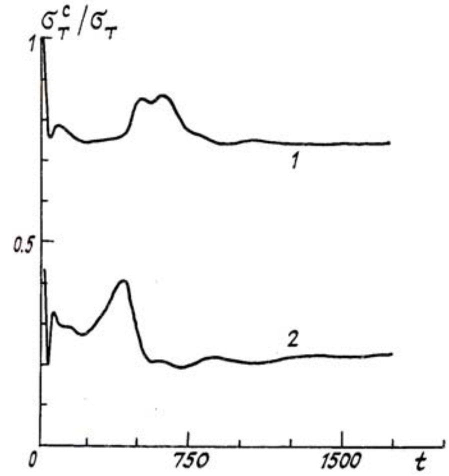

FIG. 3.

REFERENCES

1. B.P. Gerasimov, V.M. Gordienko, and A.P. Sukhorukov, Inzh. Fiz. Zh. **33**, 709–718 (1977).
2. B.P. Gerasimov, V.M. Gordienko, and A.P. Sukhorukov, Inzh. Fiz. Zh. **34**, 331–336 (1979).
3. L.D. Landau and E.M. Lifshitz, *Fluid Mechanics* (Pergamon Press, Oxford, 1959).
4. B.M. Berkovskii and V.K. Polevikov, *Numerical Experiment in Convection* (Minsk State University Press, Minsk, 1988).
5. I.Yu. Murokh, *Thermal Physics and Physical Chemistry of Power Plants* (Institute of Heat and Mass Transfer, Academy of Sciences of the Belorussian SSR, Minsk, 1986).
6. I.A. Chertkova and S.S. Chesnokov, Atm. Opt. **3**, No. 2, 108–113 (1990).
7. A.A. Samarskii and E.S. Nikolaev, *Solution Methods for Grid Equations* (Nauka, Moscow, 1978).
8. P.J. Roache, *Computational Fluid Dynamics* (Albuquerque, 1976).
9. V.A. Petrishchev, L.V. Piskunova, V.I. Talanov, and R.A. Erm, Izv. Vyssh. Uchebn. Zaved. Ser. Radiofiz. **24**, 161–171 (1981).
10. B.M. Berkovskii and E.F. Nogotov, Mekh. Zhidk. Gaza, No. 2, 147–154 (1970).
11. A. Thom and C.J. Apelt, *Field Computation in Engineering and Physics* (Van Nostrand, London, 1961).
12. L.C. Woods, Aeronaut. Quart. **5**, No. 3, 176 (1954).
13. R.C. Singleton, IEEE **AU-17**, No. 2, 93 (1969).